ADVANCED MULTIVARIATE INVERSION TECHNIQUES FOR HIGH RESOLUTION 3D GEOPHYSICAL MODELING

Monica Maceira[1], Haijiang Zhang[2], Ryan T. Modrak[1], Charlotte A. Rowe[1], and Michael L. Begnaud[1]

Los Alamos National Laboratory[1] and Massachusetts Institute of Technology[2]

Sponsored by the National Nuclear Security Administration

Award No. DE-AC52-06NA25396/LA09-3D Inv-NDD02

ABSTRACT

To meet the United States Government nuclear explosion monitoring requirements with high confidence, the Air Force Technical Applications Center needs new and improved capabilities for analyzing regional seismic, teleseismic, and infrasound event data. Recently, the National Nuclear Security Administration has decided to investigate three-dimensional (3D) modeling in an effort to further improve knowledge of the compressional and shear-velocity structure as well as reduce uncertainty and more accurately detect, locate, and identify small (body wave magnitude m_b<4) seismic events. For seismically active areas, inaccurate models can be corrected using the kriging methodology; therefore, it is possible to detect, locate, and identify large events even with limited resolution models. This is not necessarily the case for smaller events, however, and it is even more of a challenge for aseismic regions. On the other hand, improving near-regional to local monitoring demands that we address the Earth's heterogeneities and 3D complexities.

Motivated by the shortcomings of existing single-parameter inversion methods in accurate prediction of other geophysical parameters, this research was mainly focused during its first year on the development of advanced multivariate inversion techniques to generate a realistic, comprehensive, and high-resolution 3D model of the seismic structure of the crust and upper mantle that satisfies multiple independent geophysical datasets. During its second year, we have focused on the efficient implementation of the newly developed technique. Application to different areas around the globe with different sets of observations allows us to study sensitivities, trade-offs, and possible improvements of the methodology. We present 3D seismic velocity models of the crust and upper mantle beneath several regions, resulting from the simultaneous and joint use of seismic body-wave arrival times, surface-wave dispersion measurements, and gravity data. The joint inversion takes advantage of strengths of individual datasets and is able to better constrain the velocity models from shallower to greater depths. Combining three different datasets to jointly invert for the velocity structure is equivalent to a multiple-objective optimization problem. Because it is unlikely that the different "objectives" (data types) would be optimized by the same parameter choices, some trade-off between the objectives is needed. The optimum weighting scheme for different data types is based on relative uncertainties of individual observations and their sensitivities to model parameters.

OBJECTIVES

The ultimate goal of this study is to improve our knowledge of the 3D compressional and shear-velocity structure and enable us to reduce uncertainty and more accurately detect, locate, and identify small (body-wave magnitude m_b<4) seismic events, and therefore improve our capabilities for nuclear explosion monitoring (NEM). This project specifically improves seismic monitoring technology through the development and application of advanced multivariate inversion techniques to generate a realistic, comprehensive, and high-resolution 3D model of the seismic structure of the crust and upper mantle that satisfies numerous independent geophysical datasets.

RESEARCH ACCOMPLISHED

This is the second year of a three-year project. During the first year and motivated by the shortcomings of existing single-parameter inversion methods in accurate prediction of other geophysical parameters (e.g. Julià et al. 2000, 2003; Maceira, 2006; Maceira and Ammon, 2006), we focused on the development of advanced multivariate inversion techniques to generate a realistic, comprehensive, and high-resolution 3D model of the seismic structure of the crust and upper mantle that satisfies multiple independent geophysical datasets (Maceira et al, 2009). In particular, we developed a method to simultaneously and jointly invert four different datasets: surface-wave dispersion measurements, teleseismic P-wave receiver functions, gravity observations, and body wave (both P and S phases) travel-time arrivals. Surface wave dispersion measurements are primarily sensitive to seismic shear wave velocities. Theoretically, the dispersion curve is a nonlinear function of shear wave velocity and/or compressional wave velocity and density of the media (Bucher and Smith, 1971). However, it has been proved (Takeuchi and Saito, 1972; Aki and Richards, 1980) that the sensitivity to the P-wave velocity is significantly smaller than the sensitivity to the S-wave velocity. Also the sensitivity function for the density is smaller than the one for the shear-wave velocity (Bache et al., 1978; Tanimoto, 1991). Therefore, shear velocity variations are usually the model parameters in inversion studies of surface-wave dispersion. But, at shallow depths, it is difficult to obtain high resolution and constrain the structure. This is because the longer the period, the deeper the surface-wave energy penetrates, so shorter periods are primarily sensitive to upper crustal structures. But short periods are difficult to measure, especially in tectonically and geologically complex areas. On the other hand, gravity inversions have the greatest resolving power at shallow depths since gravity anomalies decrease in amplitude and increase in wavelength with increasing depth. And gravity measurements supply constraints on rock density variations. In addition, surface-wave dispersion measurements are primarily sensitive to vertical shear-wave velocity averages; while body wave receiver functions are sensitive to shear-wave velocity contrasts and vertical travel-times. Addition of the seismic travel-time data helps to constrain the shear wave velocities both vertically and horizontally in the model cells crossed by the ray paths. Thus by combining these four complimentary datasets into a single inversion, we can obtain a self-consistent 3D seismic velocity-density model with increased resolution of shallow geologic structures. Our final algorithm is a modification of the Maceira and Ammon (2009) joint-inversion code, in combination with the regional version of the double-difference (DD) tomography program *tomoDD* (Zhang and Thurber, 2003, 2006), with a fast LSQR solver operating on the gridded values jointly.

During this second year, we have focused on the efficient implementation of this newly developed technique. Application to different areas around the globe with different sets of observations allows us to study sensitivities, trade-offs, and possible improvements of the methodology. We present here 3D seismic velocity models of the crust and upper mantle beneath several regions, resulting from the simultaneous and joint use of seismic body-wave arrival times, surface-wave dispersion measurements, and gravity data.

East Africa Rift System

Knowledge of crustal and upper mantle structure is of importance for understanding East Africa's geodynamic evolution and for addressing broader questions about the causes of continental breakup. Though recent investigations have yielded improved characterizations of the rift zone, questions remain concerning the distribution of velocity anomalies (e.g., Julià et al., 2005), extent of lithospheric thinning (e.g., Weeraratne et al., 2003), and temporal variation in rift evolution (e.g., Ebinger, 1989). Key to resolving these questions are better constrained seismic models. We decided to test our joint inversion methodology in this region due to its scientific significance and because of a more practical reason: the unprecedented opportunity of getting a handle on on-land Bouguer gravity observations. Benefits of our joint inversion approach appear pronounced when working with regions of strong lateral contrast as found in central Asia (Maceira and Ammon, 2009). In applying the joint-inversion

technique to East Africa, we solve for velocity structure in an area with less lateral heterogeneity but great tectonic complexity. To increase the effectiveness of the technique in this region, we explore gravity-filtering methods and test different velocity-density relations (the relationship between the independent datasets is always one of the difficulties with simultaneous joint inversions).

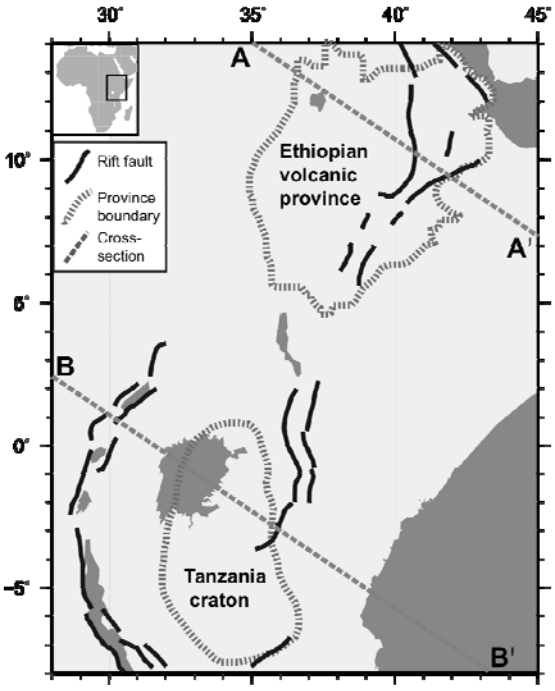

Figure 1. We distinguish between Ethiopia and Tanzania as distinct portions of the larger rift system. The Ethiopian volcanic province (after Keranen et al., 2009) spans the northern portion of the rift system. The Tanzania craton (after Nyblade and Brazier, 2002) marks the southern portion of the rift system (rift lies for the most part along the edges of the craton).

The area for the inversion spans the broad uplifted region from Ethiopia at one end to Kenya, Uganda, and Tanzania at the other (Figure 1). Near the northern boundary of our study area, the Main Ethiopia Rift meets the incipient Red Sea and Gulf of Aden spreading ridges. At the opposite end, the rift system splits into distinct western and eastern branches, which largely sidestep the Archean Tanzania craton. Recent inversions of East Africa have employed body waves (e.g., Benoit et al., 2006), surface waves (e.g., Weeraratne et al., 2003), receiver functions, or some combination of these (e.g., Julià et al., 2005; Keranen et al., 2009). Although useful comparisons can be drawn between the Ethiopian and Tanzanian portions of the rift system, most tomographic studies to date have focused exclusively on one section or the other. The current inversion, in contrast, is carried out over a wider area than most previous studies, allowing straightforward comparison between these two distinct portions of the rift system.

Fundamental-mode Rayleigh wave group velocity estimates with periods from 7 s to 150 s were obtained from Pasyanos and Nyblade (2007) for the inversion. Though less detailed than images from local seismic arrays (e.g., Prodehl et al., 1997), these estimates span a broader spatial and period range. Gravity data for the inversion were derived from the Gravity Recovery and Climate Experiment (GRACE) (Tapley et al., 2005). Comparison of GRACE-converted Bouguer anomalies with values from a proprietary gravity compilation showed close agreement between the two datasets; in light of this similarity, we chose the GRACE data because of their more uniform coverage.

We developed and implemented a method to increase the usefulness of gravity data by filtering the Bouguer anomaly map. Though commonly applied in gravity forward modeling (e.g., Simiyu and Keller, 1997) such techniques have not to our knowledge been used in previous joint inversion studies (e.g., Lees and VanDecar, 1991; Zeyen and Achauer 1997; Tiberi et al., 2003; Maceira and Ammon, 2009). Figure 2a suggests possible benefits of filtering. In this figure, results from the inversion using group velocities only (solid line) provide the starting model for the joint inversion (dashed line). Comparison of the two profiles suggests that the addition of unfiltered gravity data contributes little in the way of distinguishing between features at different depths. Rather than improving resolution at shallow depths as desired, features in the unfiltered gravity data are smeared into the mantle; moreover, within the mantle the two profiles are offset by a roughly constant amount, suggesting that gravity data provide inadequate constraints on mantle anomalies. Examination of additional profiles shows that these problems, likely exacerbated by East Africa's pronounced long-wavelength Bouguer components (Girdler, 1975), are pervasive throughout the study area. In response, we employ filtering methods to remove the long-wavelength gravity components, reducing the tendency of crustal gravity features to be smeared into the mantle. To balance the change to the observed gravity values brought on by filtering, we reduce the contribution to the predicted gravity values from blocks below 60 km, corresponding to the portion of the Bouguer anomaly signal we attempt to suppress. Finally, while allowing velocity structure above 60 km to vary freely, below 60 km we induce agreement between the joint inversion results and the initial model by imposing stronger a priori model constraints. In the application of the described technique, problems of depth correlation associated with filtering make our choice of depth cutoff (60 km) somewhat subjective. This disadvantage, however, is likely outweighed by the reduction in smearing of the gravity signal

suggested by Figure 2b. Although filtering removes potentially useful information on mantle structure, the remaining short-wavelength signal can be assigned with greater reliability within the crust, avoiding the mutually degrading effects of smearing between crust and mantle. To remove the long-wavelength components from the Bouguer gravity map, we follow Tessema and Antoine (2004), who use an upward continuation method and demonstrate correlation with crustal geology.

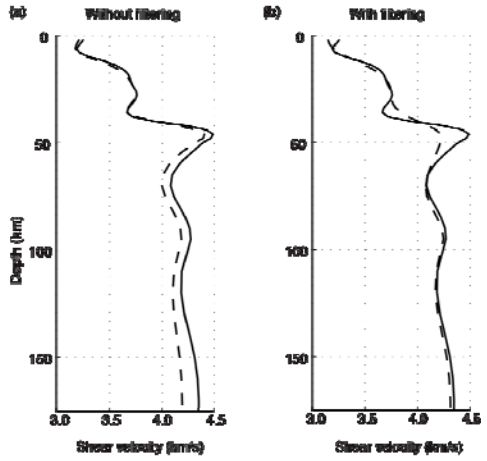

Figure 2. One-dimensional profiles from a representative cell in our model. Comparison shows results from an inversion of group velocities only (solid lines) and from joint inversion (dashed lines). (a) Without gravity filtering, results point to an inability to distinguish between density anomalies at depth. (b) With gravity filtering, the two profiles agree less closely at crustal depths and more closely over mantle depths.

Previous inversions have incorporated gravity data by formulating the forward problem in two steps: (1) velocity variations are mapped to density variations and (2) density variations are mapped to gravity anomalies. While the second mapping is mathematically straightforward, the first necessitates use of empirical formulae. Perhaps because empirical mappings between density and P-wave velocity (e.g., Birch's law) are more familiar than mappings between density and S-wave velocity, previous studies have relied on the former together with ad hoc scaling to obtain S-wave velocities. Here, we eliminate the need for such scaling by adopting a direct mapping between density and S-wave velocity. Given the variability in Poisson's ratio for rift zones (e.g., Dugda et al., 2005), this new mapping provides the proper framework for allowing spatial V_P/V_S variability, which we envision developing in future inversions.

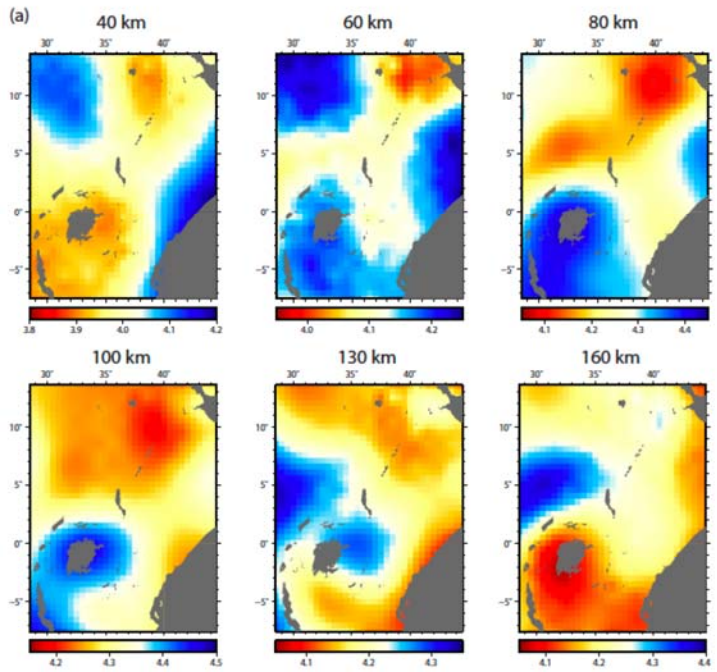

Figure 3. Horizontal cross sections at various depths through the 3D shear velocity model (velocity units: km/s).

Figure 3 shows the 3D S-wave velocity model obtained from the joint inversion. Two sets of velocity anomalies, one beneath Ethiopia and the other beneath the Tanzania craton, stand out among the most prominent features. Beneath Ethiopia a distinct low-velocity anomaly is observed over a depth of 30–150 km. Though the existence of lower-than-average shear-wave velocities in the uppermost mantle beneath Ethiopia matches a variety of previous results (e.g., Keranen et al., 2009), controversy exists regarding velocity structure at greater depths. Such disagreement may in part reflect differences in methodology. While surface wave studies (e.g., Ritsema and van Heijst, 2000) have often failed to resolve low velocities beneath Ethiopia at depths greater than 170 km, body-wave investigations (e.g., Benoit et al., 2006) have imaged low velocities extending as deep as 400 km. As a result of upward trajectories associated with incoming rays, body-wave studies may tend to underestimate velocity deviations and smear velocity structure (see Weeraratne et al., 2003, for analysis based on observations from East Africa). From these considerations, it seems likely that the true vertical extent of the low-velocity anomaly beneath Ethiopia lies between the shallower and deeper values

predicted using surface-wave and body-wave methodologies, respectively. Besides the low-velocity anomaly beneath Ethiopia, prominent velocity excursions also occur beneath Tanzania. As shown in Figure 3, we resolve high velocities below the craton over a depth of 50–130 km. Contiguous to this high-velocity zone, a low-velocity anomaly emerges at a depth of 140 km. Although the upper part of this low-velocity anomaly is well constrained by the long-period Rayleigh wave group velocities used in the inversion, sensitivity kernels suggest resolution drops off below 175 km. This juxtaposition of high and low shear-wave speeds appears consistent with the hypothesis, discussed in detail by Weeraratne et al. (2003), of a hot mantle plume impeded by cool, stable, overlying cratonic lithosphere. In the following particulars, we obtain close agreement with Weeraratne et al. (2003): (1) the low-velocity anomaly beneath the craton originates at around 140 km, (2) the anomaly lies squarely beneath the craton, and (3) deviations from background shear velocities reach as much as 5% over the depths displayed in Figure 3. Additionally, our results allow comparison between the rift structures of Ethiopia and Tanzania. In obtaining data from Pasyanos and Nyblade (2007), we use group velocities derived not only from local stations and events, but also from stations and events distributed across surrounding tectonic plates. Though the resulting continental-scale maps possess less detail than local-scale group-velocity maps, their wider spatial coverage allows straightforward comparison between distinct portions of the rift system. As a result, we find that uppermost mantle shear velocities beneath Ethiopia appear much slower than those beneath Tanzania. While the presence of shallow low velocities beneath Ethiopia can be explained in terms of lithospheric erosion or magma-assisted rifting (e.g., Dugda et al., 2007; Ebinger and Casey, 2001), the absence of shallow low velocities beneath Tanzania suggests an alternate mechanism of extension. Such differences may stem in part from inherited rheology, as related for example to the high-velocity zone observed beneath Tanzania. Finally, though a common origin below 175 km cannot be ruled out, no evidence is found to suggest the various low-velocity anomalies in Figure 3 merge continuously at depth. Indeed, low velocities beneath Ethiopia appear diffuse and diminished by 160 km, suggesting the existence of a seismic velocity discontinuity separating the low-velocity anomaly beneath Ethiopia from the one below Tanzania.

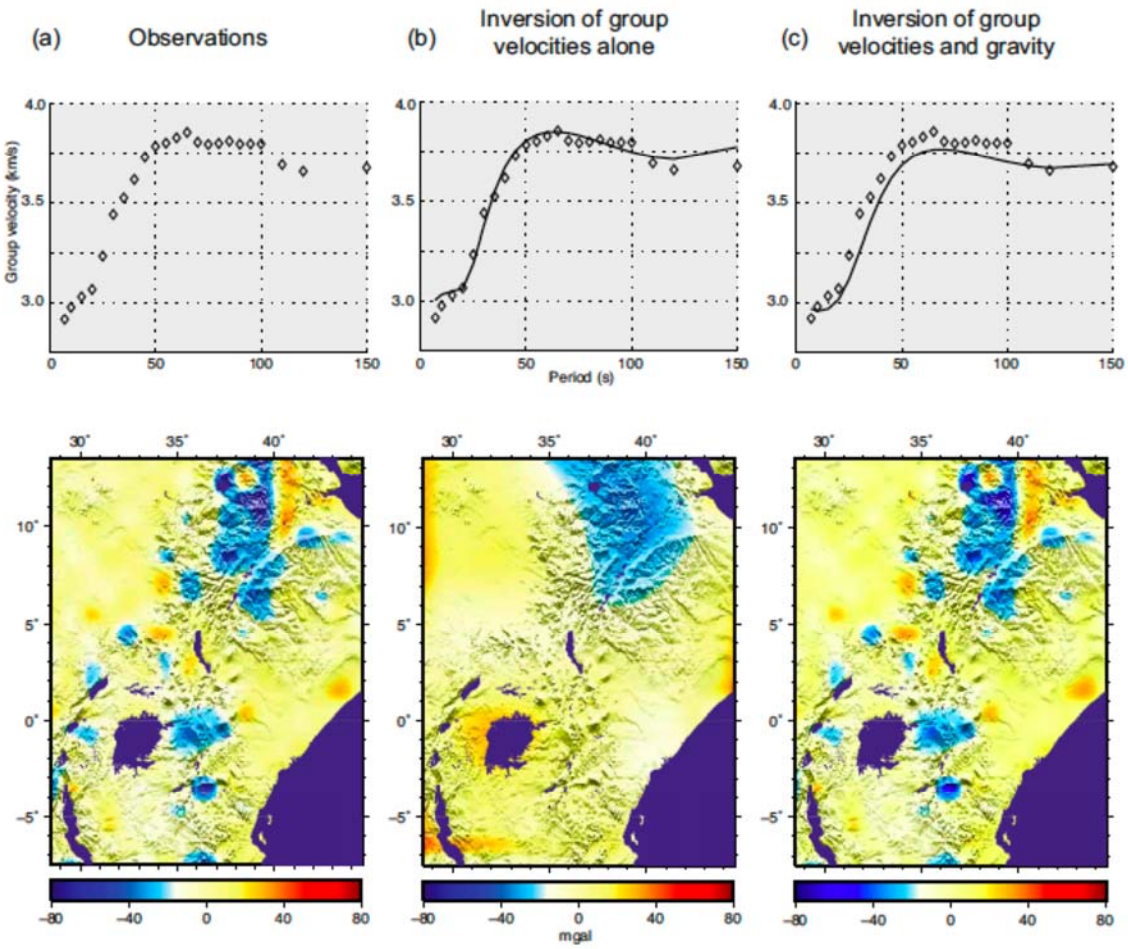

Figure 4. Fit to data from inversion of surface-wave dispersion only and from joint inversion. (a) Top: Group velocities from a representative cell in our model. Bottom: Filtered Bouguer anomalies. (b) Top: Group velocity fit obtained from the inversion of group velocities only. Bottom: Gravity fit from the same inversion. (c) Top: Group velocity fit obtained from joint inversion. Bottom: Gravity fit from joint inversion.

In the inversion carried out in central Asia by Maceira and Ammon (2009), addition of gravity data dramatically improved the fit to the Bouguer anomalies without significantly degrading the fit to the group velocities. Figure 4 demonstrates this result for the current study area as well. Although it is well known that problems of nonuniqueness make gravity data easier to match than seismic data, several observations provide confidence in our methodology's robustness. These include the simultaneous fit to both datasets shown in Figure 4 as well as other changes resulting from the addition of gravity data. Compared with results from the inversion of group velocities only, the joint-inversion methodology provides increased effectiveness in capturing Moho depth and improved resolution of uppermost mantle detail, including sharper delineation of the Tanzania craton in the vertical cross sections and in the horizontal cross section at 60 km. The resolved extent of the high-velocity cratonic region accords well with previous tomographic images (e.g., Figure 11 of Weereratne et al., 2003) and with geodynamic models suggesting strain localization in zones of weakness surrounding the craton (e.g., Nyblade and Brazier, 2002).

Utah Geothermal Field

The Cove Fort-Sulphurdale geothermal area is located in the transition zone between the Basin and Range to the west and the Colorado Plateau to the east (Figure 5). We have collected various geophysical data around the geothermal field, including heat flow (Henrikson and Chapman, 2002), gravity (Pan American Center for Earth and Environmental Studies (PACES) available at http://gis.utep.edu), seismic surface-wave phase and group velocity

maps (Yang et al., 2008), and seismic body-wave arrival times that were assembled from seismic waveforms recorded by the University of Utah Seismograph Stations (UUSS) regional network for the past 7 years and the recent EArthscope/USArray phase data. All of these geophysical datasets have different strengths for characterizing subsurface structures and properties. Combining these data through a coordinated analysis and, when possible, by joint inversion provides a detailed model of the Cove Fort geothermal region.

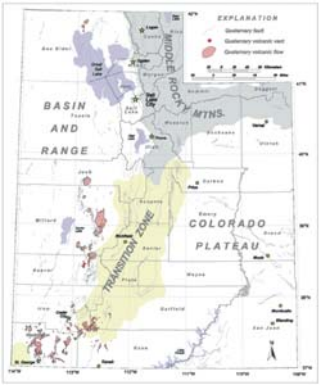

Figure 5. Utah simplified geological map (after Stokes, 1977; Hecker, 1993)

Various geophysical datasets indicate that beneath the Cove Fort-Sulphurdale geothermal resource there is a strong anomaly of low seismic velocity, low gravity, and high electrical conductivity that correlates with the high surface heat flow. This suggests that there is a heat source in the crust beneath the geothermal field. We collected first P-arrival data from more than 6500 earthquakes in the Utah region. Each event has at least six arrivals for reliably determining its location. We apply the DD seismic tomography method (Zhang and Thurber, 2003) to simultaneously determine an initial velocity structure and earthquake locations. The finite-difference travel-time calculation method of Podvin and Lecomte (1991) is used to calculate travel times between events and stations. On the preliminary regional seismic velocity map computed this way, we can also identify some other low-velocity anomalies, indicating other potential geothermal prospects. We decided to apply our joint inversion methodology to produce a better-constrained velocity structure of the Utah area, which will be very helpful for characterizing and exploring existing and potential geothermal reservoirs in the area.

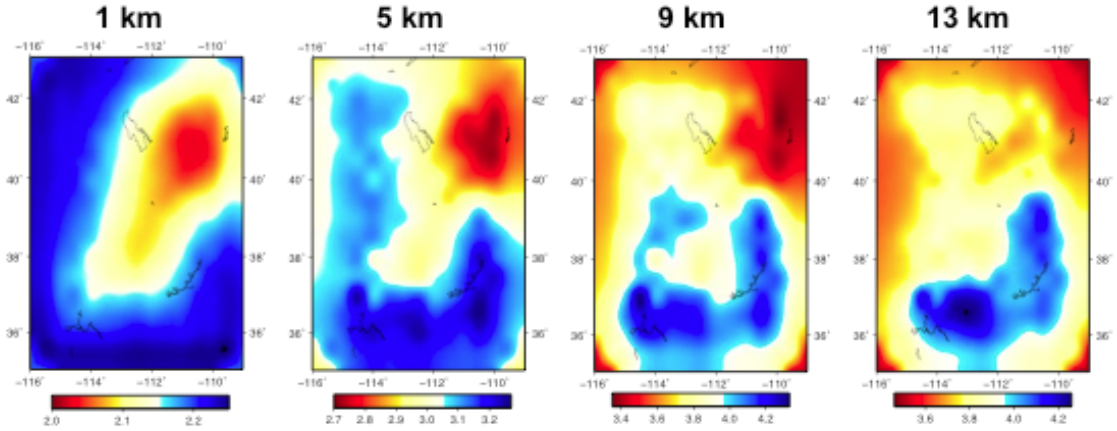

Figure 6. Shear-wave velocity model at constant depth slices. The depth of each image is shown at the top of each map (velocity units: km/s).

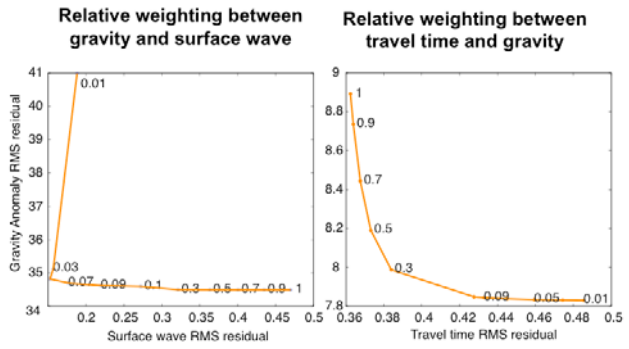

Figure 7. Trade-off curves between surface-wave and gravity data residuals (left) and between travel time and gravity data residuals (right).

Figure 6 shows the results from using the surface and gravity data to jointly determine the shear-velocity (Vs) model. Combining both datasets to jointly invert for the velocity structure is equivalent to a multiple-objective optimization problem. Because it is unlikely that the different "objectives" (data types) would be optimized by the same parameter choices, some trade-off between the objectives is needed. The optimum weighting scheme for different data types is based on relative uncertainties of individual observations and their sensitivities to model parameters. Here we determine their relative weightings through a trade-off analysis of surface-wave residual and gravity data residual (Figure 7). As a result, the model optimally fits both the surface wave and gravity data. In this study, the surface wave is weighted 50 times of the gravity data (1:0.02). Compared to the inversion using only the surface wave data, at shallow depths (e.g., 1 and 5 km), the Vs model better delineates the low-velocity anomaly. The first-order horizontal and vertical smooth weighting are also applied to constrain the model during the joint inversion. After three iterations of joint inversion, the surface-wave data residual is close to zero and the gravity data residual decreases ~90%.

Preliminary joint inversion results using seismic travel time and gravity data (Figure 8) indicate strong low velocity anomalies in middle crust beneath some known geothermal sites in Utah.

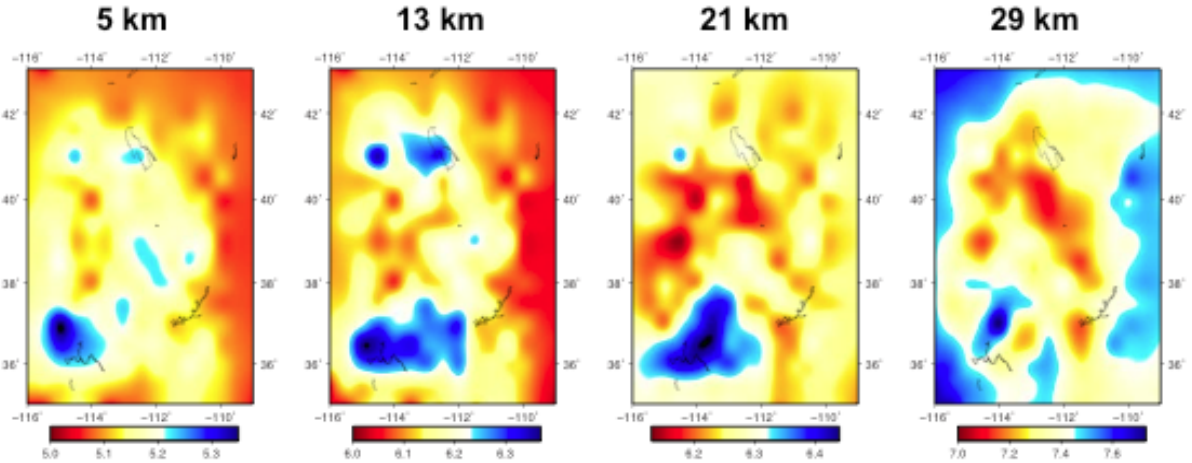

Figure 8. Compressional wave velocity model at constant depth slices. The depth of each image is shown at the top of each map (velocity units: km/s).

CONCLUSIONS AND RECOMMENDATIONS

This is the second year of a three-year project to map the 3D seismic structure of the crust and upper mantle using simultaneous joint inversion of surface-wave dispersion, gravity, receiver function, and travel-time observations. Geophysical models play an important role in ground-based nuclear explosion monitoring (GNEM). To more confidently and accurately detect, locate, and identify small seismic events, better high-resolution 3D structural models are needed. Therefore, the ongoing research directly addresses this challenge, and our results are also of fundamental importance for understanding the geodynamic evolution and formation of continents, as well as the processes acting within and on the continental lithosphere.

We are now focusing on developing 3D models for different areas for which we have different sets of observations. This approach allows us to study sensitivities, trade-offs, and possible improvements of our methodology. We have presented here models obtained for the East Africa Rift System and the Utah geothermal area (more areas of interest to the GNEM program will be shown at the MRR 2010 meeting). By tailoring our methodology to these two different areas, we have learned that besides enhancing resolution at short wavelengths, use of filtered gravity anomalies may help distinguish between anomalies at different depths. We have also tested different relations between seismic velocities and density and concluded that a relation where no a priori Poisson's ratio assumptions are needed (e.g., D. G. Harkrider's) is more beneficial. Future work will involve validation of these 3D models through the use of the spectral element method and full waveform comparisons.

ACKNOWLEDGEMENTS

Special thanks to Cindy Ebinger for kindly providing us with her gravity measurements. We thank Mike Pasyanos for allowing us to use their tomographic maps for this research. Special thanks also to D. G. Harkrider for providing us with valuable relationships between seismic velocities and density. Thanks to Chuck Ammon for valuable insights. We thank the scientists, engineers, and technicians that have created the seismic recording systems and networks that provide excellent broadband seismic observations. In particular, we thank the USGS and the IRIS Consortia (NSF) who share information and data with the global community in an effective and efficient manner. Thanks to Paul Wessel and Walter Smith (1995) for developing and maintaining their Generic Mapping Tool (GMT) that we use to create many of the illustrations used in our research. Our thanks to M. Wetovsky for editorial assistance.

REFERENCES

Aki, K. and P. G. Richards (1980*). Quantitative Seismology: Theory and Methods*, San Francisco, CA: W. H. Freeman.

Bache, T. C., W. L. Rodi, and D. G. Harkrider (1978). Crustal structures inferred from Rayleigh-wave signatures of NTS explosions, *Bull. Seismol. Soc. Am.* 68: 1399–1413.

Benoit, M. H., A. A. Nyblade, and J. C. VanDecar (2006). Upper mantle P-wave speed variations beneath Ethiopia and the origin of the Afar hotspot, *Geology* 34: 329–332.

Bucher, R. L. and R. B. Smith (1971). Crustal structure of the eastern Basin and Range province and the northern Colorado Plateau from phase velocities of Rayleigh waves, in *The Structure and Physical Properties of the Earth's Crust*, Geophysical Monograph. Series, Vol. 14, J. G. Heacock, Ed. Washington, D.C.: AGU.

Dugda, M. T., A. A. Nyblade, and J. Julià (2007). Thin lithosphere beneath the Ethiopian Plateau revealed by a joint inversion of Rayleigh wave group velocities and receiver functions, *J. Geophys. Res*. 112: B08305, doi:10.1029/2006JB004918.

Dugda, M. T., A. A. Nyblade, J. Julià, C. A. Langston, C. J. Ammon, and S. Simiyu (2005). Crustal structure in Ethiopia and Kenya from receiver function analysis: Implications for rift development in eastern Africa, *J. Geophys. Res.* 110: B01303, doi:10.1029/2004JB003065.

Ebinger, C. J. and M. Casey (2001). Continental breakup in magmatic provinces: An Ethiopian example, *Geology*, 29: 527–530.

Ebinger, C. J. (1989). Tectonic development of the western branch of the East African rift system, *Geol. Soc. Am. Bull.* 101: 885–903.

Girdler, R. W. (1975). The great negative Bouguer anomaly over Africa, *EOS Trans. AGU* 56: 516–519.

Hecker, S. (1993). Quaternary tectonics of Utah with emphasis on earthquake-hazard characterization, Utah Geological and Mineral Survey Bulletin 127.

Henrikson, A. and D. S. Chapman, 2002. Terrestrial heat flow in Utah, open report, Dept. of Geology and Geophysics, Univ. Utah.

Julià, J., C. J. Ammon, R. B. Herrmann, and A. M. Correig (2000). Joint inversion of receiver function and surface wave dispersion observations, *Geophys. J. Int*. 143: 99–112.

Julià, J., C. J. Ammon, and R. B. Herrmann (2003). Lithospheric structure of the Arabian shield from the joint inversion of receiver functions and surface wave dispersion, *Tectonophys.* 371: 1–21.

Julià, J., C. J. Ammon, and A. A. Nyblade (2005). Evidence for mafic lower crust in Tanzania, East Africa, from joint inversion of receiver functions and Rayleigh wave dispersion velocities, *Geophys. J. Int.* 162: 555–569.

Keranen, K. M., S. L. Klemperer, J. F. Lawrence, J. Julia, and A. A. Nyblade (2009). Low lower crustal velocity across Ethiopia: Is the Main Ethiopian Rift a narrow rift in a hot craton? *Geochemistry, Geophysics, Geosystems* 10: 121.

Lees, J. M. and J. C. VanDecar (1991). Seismic tomography constrained by Bouguer gravity anomalies: Applications in western Washington, *Pure Appl. Geophys*. 135: 31–52.

Maceira, M. (2006). Surface waves, Earth structure, and seismic discrimination, Ph.D. thesis, Pennsylvania State University.

Maceira, M. and C. J. Ammon (2006). Joint inversion of surface wave velocity and gravity observations and its application to Central Asian basins shear velocity structure, *Seismol. Res. Lett*. 77: 297.

Maceira, M. and C. J. Ammon (2009). Joint inversion of surface wave velocity and gravity observations and its application to Central Asian basins shear velocity structure, *J. Geophys. Res*. 114: B02314, doi:10.1029/2007JB005157.

Maceira, M., C. Rowe, H. Zhang, R. Modrak, M. Begnaud, L. Steck, G. Randall, and X. Yang (2009). Advanced Multivariate Inversion Techniques for High Resolution 3D Geophysical Modeling, in *Proceedings of the 2009 Monitoring Research Review: Ground-Based Nuclear Explosion Monitoring Technologies*, LA-UR-09-05276, Vol. 1, pp. 121–130.

Nyblade, A. A. and R. A. Brazier (2002). Precambrian lithospheric controls on the development of the East Africa rift system, *Geology* 30: 755–758.

Pasyanos, M. E. and A. A. Nyblade (2007). A top to bottom lithospheric study of Africa and Arabia, *Tectonophys.* 444: 27–4.

Podvin, P. and I. Lecomte (1991). Finite difference computation of travel times in very contrasted velocity models: A massively parallel approach and its associated tools, *Geophys. J. Int*. 105: 27–84.

Prodehl, C., J. R. R. Ritter, J. Mechie, G. R. Keller, M. A. Khan, B. Jacob, K. Fuchs, I. O. Nyambok, J. D. Obel, and D. Riaroh (1997). The KRISP 94 lithospheric investigation of southern Kenya—the experiments and their main results, *Tectonophys.* 278: 121–147.

Ritsema, J. and H. van Heijst (2000). New seismic model of the upper mantle beneath Africa, *Geology* 28: 63–66.

Simiyu, S. M. and G. R. Keller (1997). An integrated analysis of lithospheric structure across the East Africa plateau based on gravity anomalies and recent seismic studies, *Tectonophys.* 278: 291–313.

Stokes, W. L. (1977). Subdivisions of the major physiographic provinces in Utah, *Utah Geol. 4* 1: 1–17.

Takeuchi, H. and M. Saito (1972). Seismic surface waves, in *Methods of Computational Physics*, B. A. Bolt, Ed. New York, NY: Academic.

Tanimoto, T. (1991), Waveform inversion for three-dimensional density and S-wave structure, *J. Geophys. Res.* 96: 8167–8189.

Tapley, B. D., S. Bettadpur, J. C. Ries, P. F. Thompson, and M. M. Watkins (2005). GRACE measurements of mass variability in the Earth system, *Science* 305: 503–505.

Tessema, A. and L. A. G. Antoine (2004). Processing and interpretation of the gravity field of the East African Rift: Implication for crustal extension, *Tectonophys*. 394: 87–110.

Tiberi, C., M. Diament, J. Déverchère, C. Petit-Mariani, V. Mikhailov, S. Tikhhotsky, and U. Achauer (2003). Deep structure of the Baikal rift zone revealed by joint inversion of gravity and seismology, *J. Geophys. Res*. 108: B3, 2133, doi:10.1029/2002JB001880.

Weeraratne, D. S., D. W. Forsyth, and K. M. Fischer (2003). Evidence for an upper mantle plume beneath the Tanzanian craton from Rayleigh wave tomography, *J. Geophys. Res*. 108: 2427, doi:10.1029/2002JB002273.

Wessel, P. and W. H. F. Smith (1995). New version of the Generic Mapping Tools released, *EOS Trans. AGU* 76: 329.

Yang, Y., M. H. Ritzwoller, F.-C. Lin, M. P. Moschetti, and N. M. Shapiro (2008). Structure of the crust and uppermost mantle beneath the western United States revealed by ambient noise and earthquake tomography, *J. Geophys. Res*. 113: B12310, doi:10.1029/2008JB005833.

Zeyen, H. and U. Achauer (1997). Joint inversion of teleseismic delay times and gravity anomaly data for regional structures, in *Upper Mantle Heterogeneities from Active and Passive Seismology*, K. Fuchs Ed. Dordrecht, Netherlands: Kluwer Academic Publishers.

Zhang, H. and C. Thurber (2006). Development and applications of double-difference tomography, *Pure App. Geophys.* 16:, 373–03, doi:10.1007/s00024-005-0021-y.

Zhang, H. and C. H. Thurber (2003). Double-difference tomography: The method and its application to the Hayward Fault, California, *Bull. Seism. Soc. Am.* 93: 1875–1889.